

PREPARED FOR SUBMISSION TO JHEP

# Enhanced Higgs pair production from higgsino decay at the HL-LHC

Jianpeng Dai,<sup>a,b</sup> Tao Liu,<sup>c,b</sup> Daohan Wang,<sup>a,b</sup> Jin Min Yang<sup>a,b</sup>

<sup>a</sup>*CAS Key Laboratory of Theoretical Physics, Institute of Theoretical Physics, Chinese Academy of Sciences, Beijing 100190, P. R. China*

<sup>b</sup>*School of Physical Sciences, University of Chinese Academy of Sciences, Beijing 100049, P. R. China*

<sup>c</sup>*Institute of High Energy Physics, Chinese Academy of Sciences, Beijing 100049, P. R. China*  
*E-mail: [daijianpeng@mail.itp.ac.cn](mailto:daijianpeng@mail.itp.ac.cn), [liutao86@ihep.ac.cn](mailto:liutao86@ihep.ac.cn), [wangdaohan@mail.itp.ac.cn](mailto:wangdaohan@mail.itp.ac.cn), [jmyang@itp.ac.cn](mailto:jmyang@itp.ac.cn)*

**ABSTRACT:** The scenario of multi-sector SUSY breaking predicts pseudo-goldstinos which are not absorbed by the gravitino and their mass can be as low as  $\mathcal{O}(0.1)$  GeV. Since the interactions of pseudo-goldstinos are not so weak as gravitino, a produced higgsino can decay to a pseudo-goldstino plus a Higgs boson inside the detector at the LHC, and thus the higgsino pair production can lead to the signal of Higgs pair plus missing energy. For the scenario of natural SUSY which requires rather light higgsinos, such events may sizably outnumber the Higgs pair events predicted by the SM and be accessible at the HL-LHC (14 TeV with a luminosity of  $3 \text{ ab}^{-1}$ ). In this work we examine the observability of such Higgs pair plus missing energy from the decay of light higgsinos produced at the HL-LHC. Considering three channels of the Higgs-pair decay ( $bbWW^*$ ,  $bb\gamma\gamma$ ,  $bbbb$ ), our detailed Monte Carlo simulations for the signal and backgrounds show that the best channel is  $bbbb + \cancel{E}_T$ , whose statistical significance can reach  $5\sigma$  for a light higgsino allowed by current experiments. This is significantly over the SM Higgs pair result which is about  $1.8\sigma$ .

---

## Contents

<b>1</b>	<b>Introduction</b>	<b>1</b>
<b>2</b>	<b>A description of theoretical framework</b>	<b>2</b>
<b>3</b>	<b>Observability at the HL-LHC</b>	<b>5</b>
3.1	The signal of $hhG'G' \rightarrow b\bar{b}WW^*G'G' \rightarrow b\bar{b}\ell^+\ell^- + \cancel{E}_T$	6
3.2	The signal of $hhG'G' \rightarrow b\bar{b}b\bar{b} + \cancel{E}_T$	8
3.3	The signal of $hhG'G' \rightarrow b\bar{b}\gamma\gamma + \cancel{E}_T$	12
<b>4</b>	<b>Conclusion</b>	<b>15</b>

---

## 1 Introduction

The precision test of the Higgs properties and the exploration of new physics beyond the standard model (SM) is the main task of the Large Hadron Collider (LHC) and other future colliders after the Higgs boson was discovered in 2012. Now the Higgs mass has already been measured to an impressive precision, and in order to confirm the mechanism of electroweak symmetry breaking described in the SM and probe possible new physics beyond the SM, the Higgs self-coupling  $\lambda_{hhh}$  has to be reconstructed by experimental measurements which requires the production of at least two Higgs bosons at the LHC. In the SM, the dominant channel for Higgs pair production at the LHC is the gluon fusion channel, in which these two Higgs bosons could be directly radiated from heavy quark loops or from a virtual Higgs boson through the self-coupling  $\lambda_{hhh}$ . Comparing with the single Higgs production, the Higgs pair processes are additionally suppressed by the destructive interference between the above two contributions. The cross sections for Higgs pair production is about three orders of magnitude smaller than the single Higgs production, and thus it cannot reach the observable level when considering the huge QCD background at the LHC. On the experimental side, ATLAS and CMS have published measurements of Higgs pair production in the decay channels  $b\bar{b}WW^*$  [1, 2],  $b\bar{b}b\bar{b}$  [3, 4],  $b\bar{b}\gamma\gamma$  [5, 6],  $b\bar{b}\tau^+\tau^-$  [7, 8] and  $WW^*WW^*$  [9], and the combination of different measurements gives a constraint on the trilinear self-coupling,  $-5.0 < \lambda_{hhh}/\lambda_{hhh}^{SM} < 12.0$  at 95% C.L. [10], with the assumption that all other couplings

are SM-like. The high-luminosity run of the LHC will further narrow the window of  $\lambda_{hhh}$ .

The Higgs pair production rate could be altered in new physics models (see, for examples Refs. [11–27] and references therein) which may predict different Higgs self-coupling from the SM, e.g., in the next-to-minimal supersymmetric model (NMSSM) or little Higgs theory, the Higgs self-coupling may be significantly different from the SM value [28–30]. Of course, the Higgs pair events may also come from the decays of the new particles predicted in new physics models. In this work we consider supersymmetric models with multi-sector SUSY breaking, in which each breaking sector provides a massless goldstino  $\eta_i$  at tree level with SUSY breaking scale  $F_i$ . When taking into account radiative corrections, the true goldstino which will be absorbed by gravitino remains massless, while the pseudo-goldstino acquires non-vanishing contribution and obtains a mass [31, 32]. Unconstrained by the supercurrent like gravitino, the interaction between pseudo-goldstino and visible fields could be strong enough and thus may lead to unconventional phenomenology [31–44]. In our previous studies [40–42] we found that the lightest neutralino could be bino-like and mainly decay to Higgs or longitudinal  $Z$  boson plus pseudo-goldstino while the lightest chargino may decay to  $W$  boson plus pseudo-goldstino. In those studies only the decay channels to  $Z$  or  $W$  boson are considered since they are easier to detect. In case that the lightest neutralino is higgsino-like and dominantly decays to Higgs plus pseudo-goldstino, the production of higgsino-like neutralinos will lead to the signal of Higgs pair plus missing energy. Note that as fermions the higgsino-like neutralinos may be more copiously produced than the Higgs bosons. The Higgs pair events from these neutralino decays may sizably outnumber the Higgs pair events predicted by the SM. In addition, the accompanied large missing energy may help to reduce the QCD backgrounds. In this work we perform a comprehensive study for this Higgs channel at the high luminosity LHC (HL-LHC). We will work in the natural SUSY scenario which predicts light higgsinos, and consider three typical Higgs-pair decay channels to study the observability, i.e.,  $b\bar{b}WW^*$  with  $W$  boson decaying leptonically,  $b\bar{b}b\bar{b}$  and  $b\bar{b}\gamma\gamma$ .

This work is organized as follows. In Sect. 2 we make a brief review on pseudo-goldstino and mention some related theoretical basics. Then in Sect. 3 we perform a Monte Carlo simulation for the signal and backgrounds for three decay channels for the Higgs pair. The conclusion is made in Sect. 4.

## 2 A description of theoretical framework

In the scenario of multi-sector SUSY breaking, each hidden sector with spontaneous SUSY breaking at scale  $F_i$  could be parameterized in a non-linear way  $X_i = \eta_i^2/(2F_i) +$

$\sqrt{2}\theta\eta_i + \theta^2 F_i$ , where  $\eta_i$  denotes the so-called goldstino. Then the soft terms for the visible superfields can be obtained through the non-trivial Kähler potential  $K$  and gauge kinetic function  $f$

$$K = \Phi^\dagger \Phi \sum_i \frac{m_{\phi,i}^2}{F_i^2} X_i^\dagger X_i, \quad (2.1)$$

$$f_{ab} = \frac{1}{g_a^2} \delta_{ab} \left( 1 + \sum_i \frac{2m_{a,i}}{F_i} X_i \right). \quad (2.2)$$

Here  $m_{\phi,a}$  are the soft masses for the chiral superfields and gauginos, respectively. Other soft trilinear  $A$  terms and bilinear  $B_\mu$  which will not be used in the following discussion could also be easily constructed. Take the scenario of two hidden sectors as an example, with the definition  $F = \sqrt{F_1^2 + F_2^2}$  and  $\tan \theta = F_2/F_1$ ,  $G = \eta_1 \cos \theta + \eta_2 \sin \theta$  would be absorbed by gravitino through the super-Higgs mechanism and  $G' = -\eta_1 \sin \theta + \eta_2 \cos \theta$  is left as the physical pseudo-goldstino. Then one can obtain the interaction between  $G, G'$  and visible particles up to order  $1/F_i$

$$\mathcal{L}_G = \frac{m_\phi^2}{F} G \psi \phi^* - \frac{im_a}{\sqrt{2}F} G \sigma^{\mu\nu} \lambda^a F_{\mu\nu}^a + \frac{m_a}{F} G \lambda^a D^a, \quad (2.3)$$

$$\mathcal{L}_{G'} = \frac{\tilde{m}_\phi^2}{F} G' \psi \phi^* - \frac{i\tilde{m}_a}{\sqrt{2}F} G' \sigma^{\mu\nu} \lambda^a F_{\mu\nu}^a + \frac{\tilde{m}_a}{F} G' \lambda^a D^a. \quad (2.4)$$

Through the definition of  $m_{a,\phi}$  and  $\tilde{m}_{a,\phi}$

$$\begin{aligned} m_a &= m_{a,1} + m_{a,2}, & \tilde{m}_a &= -m_{a,1} \tan \theta + m_{a,2} \cot \theta, \\ m_\phi^2 &= m_{\phi,1}^2 + m_{\phi,2}^2, & \tilde{m}_\phi^2 &= -m_{\phi,1}^2 \tan \theta + m_{\phi,2}^2 \cot \theta, \end{aligned} \quad (2.5)$$

it is easy to see that pseudo-goldstino  $G'$  could couple to ordinary fields in a total different way compared with gravitino. Under the condition of approximately vanishing  $\tilde{m}_a$ , the lightest neutralino could only decay to Higgs or longitudinal  $Z$  boson plus  $G'$ . The details about the derivation as well as the corresponding dynamical realization of this condition from the viewpoint of model-buildings could be found in our previous paper [41].

Obviously the mass of  $G'$  is a crucial parameter for phenomenological analysis. At tree level  $G'$  acquires contribution which is just twice the gravitino mass  $m_{3/2}$  via supergravity [33]. The leading order correction without gravitational effect arise at three-loop level. When the two messenger scales are equal, the loop correction is at the order of GeV scale [31]. And through an explicit analytical calculation, we found that this correction could be as low as  $\mathcal{O}(0.1)$  GeV if one messenger mass is 100 times larger

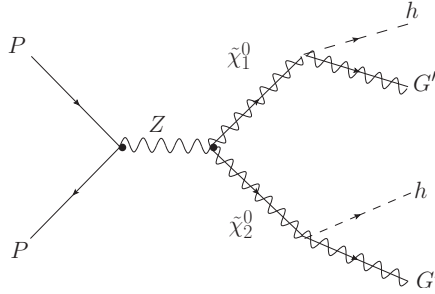


**Figure 1.** The Feynman diagram for the Higgs pair event from the decay of higgsinos produced at the LHC

than the other [32]. In our following Monte Carlo simulations the pseudo-goldstino mass is fixed to a reasonable value of 0.5 GeV.

Next, let us turn to the visible sector and have a close look at neutralino pair production. The property of the neutralinos depends heavily on the choice of certain parameters in the minimal supersymmetric model (MSSM). Since our aim is to study the Higgs phenomenology arising from pseudo-goldstino, we choose the scenario of natural SUSY [45–50] which predicts light higgsinos. In this scenario the higgsinos are rather light, i.e.,  $\mu$  is assumed to be 100-300 GeV, while the gauginos are much heavier. So the neutralinos  $\tilde{\chi}_1^0$  and  $\tilde{\chi}_2^0$  are highly higgsino-like and nearly degenerate in masses. Then at the LHC the productions of any pair of them just give missing energy in the MSSM. In order to detect their productions, a hard jet radiated from initial partons is usually required and the signal of monojet plus missing energy is searched, which is found to be rather challenging at the LHC [51] (a global likelihood analysis of the electroweakino sector shows that no range of neutralino or chargino masses can be robustly excluded by current LHC searches [52]). Now with multi-sector SUSY breaking, the higgsino-like  $\tilde{\chi}_1^0$  and  $\tilde{\chi}_2^0$  could decay to Higgs boson plus pseudo-goldstino, and their pair productions can lead to the signal of Higgs pair plus missing energy.

For the pair productions of  $\tilde{\chi}_1^0$  and  $\tilde{\chi}_2^0$  at the LHC, the cross-section of  $\tilde{\chi}_1^0\tilde{\chi}_2^0$  production is much larger than  $\tilde{\chi}_1^0\tilde{\chi}_1^0$  and  $\tilde{\chi}_2^0\tilde{\chi}_2^0$ . Thus

$$pp \rightarrow \tilde{\chi}_1^0\tilde{\chi}_2^0 \rightarrow hhG'G' \quad (2.6)$$

is considered in our study. The corresponding Feynman diagram of the signal is shown in Fig. 1. To get the mass spectrum and the corresponding mixing matrices for the neutralinos, SOFTSUSY [53] is used in our calculation. Here the mass of the SM-like Higgs boson is fixed at 125 GeV,  $\mu$  is assumed to have a positive sign and the value of

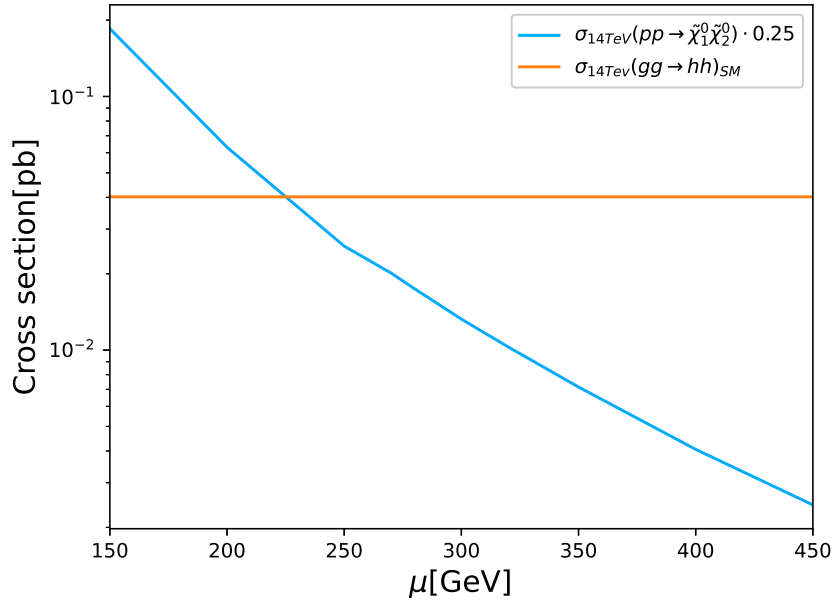


**Figure 2.** The Higgs pair cross section from  $\tilde{\chi}_1^0 \tilde{\chi}_2^0$  production at the 14 TeV LHC at next-to-leading order, compared with the SM Higgs pair cross-section at NLO [54].

$\tan \beta$  is chosen to be 10. In addition, we fix soft gaugino masses as  $M_1 = 1$  TeV and  $M_2 = 1$  TeV.

Before discussing the role of missing energy from pseudo-goldstino in distinguishing signal from backgrounds, in Fig. 2 we show the total cross sections for Higgs pair produced through higgsino decay in natural SUSY, compared with the SM Higgs pair cross-section at NLO [54]. For the couplings between higgsinos and pseudo-goldstino, we use an effective way to study the phenomenology as in the literature [41] and assume that the branching ratio of higgsino decay to Higgs to be 1/2 throughout this paper. So we see that for light higgsinos the Higgs pair produced from higgsino decay may have a larger cross section than the SM Higgs pair.

### 3 Observability at the HL-LHC

In this section we study in detail the signal of Higgs pair plus missing energy from higgsino decay in natural SUSY. Signal and the background processes are modeled using simulated Monte Carlo event samples by MadGraph5\_aMC@NLO2.4.2 [55] with the default NNPDF2.3QED parton distribution functions [56] at the  $\sqrt{s} = 14$  TeV LHC. The cross section of higgsino production is normalized to NLO with the help of

Prospino2 [57]. The pseudo-goldstino interaction is implemented in FeynRules [58] and the UFO model file [59] is passed to MadGraph5. We use PYTHIA8.205 [60] program to describe the parton-shower and hadronization.

The fast detector simulations are performed by Delphes [61] with the ATLAS detector. Using FastJet [62] for jet-reconstruction with the anti- $k_T$  algorithm [63], fixing a cone size of  $R=0.4$  for a jet (the situation of  $bbbb$  channel will be further discussed in the following subsection), we include detector effects relevant for the HL-LHC, where jets and leptons are smeared according to their energies. For the analysis, we consider jets with  $p_{Tj} > 20$  GeV and  $|\eta_j| < 2.5$ , and use the flat  $b$ -tagging efficiency  $\epsilon_{b \rightarrow b} = 0.75$  and the flat mis-tagging rates for non- $b$  jets  $\epsilon_{c \rightarrow b} = 0.1$  and  $\epsilon_{j \rightarrow b} = 0.01$  [64]. As for leptons, we require  $P_T^\ell / \sum P_T > 0.7$  with  $P_T^\ell > 20$  GeV and  $|\eta_\ell| < 2.5$  within  $\Delta R = 0.3$ .

### 3.1 The signal of $hhG'G' \rightarrow b\bar{b}WW^*G'G' \rightarrow b\bar{b}\ell^+\ell^- + \cancel{E}_T$

We first study the channel  $hhG'G' \rightarrow b\bar{b}WW^*G'G' \rightarrow b\bar{b}\ell^+\ell^- + \cancel{E}_T$ . The branching ratio of  $h \rightarrow WW^*$  is the second largest, next to  $h \rightarrow b\bar{b}$ . Considering all relevant branching fractions, our signal cross section is  $\frac{1}{2} \cdot \sigma_{\tilde{\chi}_1^0 \tilde{\chi}_2^0} \cdot BR(h \rightarrow WW^* \rightarrow \ell^+\ell^-\nu\bar{\nu}) \cdot BR(h \rightarrow b\bar{b})$ , where  $\ell$  denotes an electron or a muon, including leptons from tau decay. Because our signal is similar to SM Higgs pair channels, so we can refer to their backgrounds [65]. The major background is  $t\bar{t}$  production, whose NNLO QCD cross-section is 953.6 pb [66]. The second large background is  $t\bar{t}h$ , whose NLO QCD cross-section is 611.3 fb [67]. For the  $t\bar{t}V$  ( $V = W^\pm, Z$ ) backgrounds, we apply an NLO k-factor of 1.54 and obtain a cross-section of 1.71 pb [68]. We also apply a k-factor of 1.0 for the Drell-Yan type background  $\tau\tau b\bar{b}$ . Finally, we generate  $tW^\pm j$  events (in the five flavor scheme), whose overlap with  $t\bar{t}$  should be subtracted. To reconstruct events, the off-shell effects for the top quark and  $W$  boson need to be considered properly.

We employ the following cuts at parton level:  $p_{Tj} > 20$  GeV,  $p_{Tb} > 20$  GeV,  $p_{T\gamma} > 10$  GeV,  $p_{T\ell} > 10$  GeV,  $|\eta_j| < 5$ ,  $|\eta_b| < 5$ ,  $|\eta_\gamma| < 2.5$ ,  $|\eta_\ell| < 2.5$ ,  $\Delta R_{bb} < 1.8$ ,  $\Delta R_{\ell\ell} < 1.3$ ,  $70 \text{ GeV} < m_{jj}, m_{bb} < 160 \text{ GeV}$  and  $m_{\ell\ell} < 75 \text{ GeV}$ . For  $tW^\pm j$  backgrounds, we impose  $5 \text{ GeV} < m_{\ell\ell} < 75 \text{ GeV}$  additionally. Here the angular distance  $\Delta R_{ij}$  is defined by

$$\Delta R_{ij} = \sqrt{(\Delta\phi_{ij})^2 + (\Delta\eta_{ij})^2}, \quad (3.1)$$

where  $\Delta\phi_{ij} = \phi_i - \phi_j$  and  $\Delta\eta_{ij} = \eta_i - \eta_j$  are respectively the differences of the azimuthal angles and rapidities between particles  $i$  and  $j$ .

We set a sequence of event selections. From Fig. 3 we can find that the distributions of  $\Delta R_{\ell\ell}$ ,  $\Delta R_{bb}$ ,  $m_{bb}$ ,  $m_{\ell\ell}$  and  $\cancel{E}_T$  are different between the signal and the backgrounds, and thus we use them to make further cuts. Since the  $P_T$  distributions of backgrounds

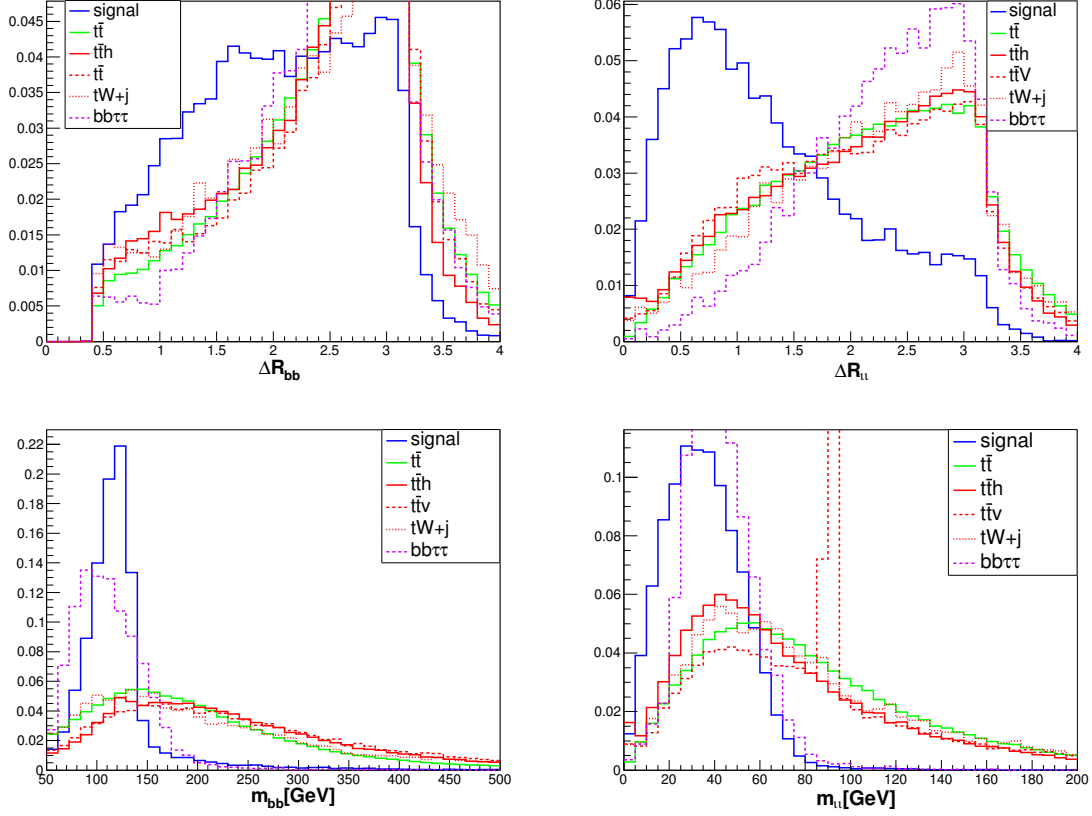


**Figure 3.** Distribution of the  $\mu = 150$  GeV for signal and different types of backgrounds after basic cuts. The  $y$ -axis represents the normalized number of events for each process.

and signal have no obvious difference, we simply set  $P_{Tl} > 20$  GeV and  $P_{Tb} > 30$  GeV. The cuts  $\Delta R_{ll} < 1.0$  and  $\Delta R_{bb} < 1.0$  are imposed to highly suppress the backgrounds. We make use of invariant masses of leptons and  $b$ -jets to suppress backgrounds, because the pair of  $b$ -jets is reconstructed near the Higgs boson mass. From a further analysis of the signal and background features, we find that the missing energy of  $t\bar{t}$  is quite approaching to the signal, and thus we gradually increase the cuts of  $\cancel{E}_T$  to find the best value. Finally, we find that  $\cancel{E}_T > 120$  GeV can most efficiently cut the  $t\bar{t}$  and  $t\bar{t}h$  backgrounds. The detailed results are shown in Table 1.

With the above analysis, we can summarize the sequence of cuts as follows:

- The two leading jets must be  $b$ -tagged, each with  $P_T > 30$  GeV;
- Exactly two isolated leptons of opposite sign, each with  $P_{Tl} > 20$  GeV;



**Table 1.** Signal and background cross sections in units of fb after baseline cuts (first row) and at different stages of analysis, using a combination of kinematic variables and requiring the events number  $N > 10$ . The significance  $\sigma$  is calculated using the Poisson formula for a luminosity of  $3 \text{ ab}^{-1}$  at the 14 TeV LHC.

Cuts	signal	$t\bar{t}$	$t\bar{t}h$	$t\bar{t}V$	$tW + j$	$b\bar{b}\tau^+\tau^-$	$\sigma$	$S/B$
$P_{T\ell} > 20 \text{ GeV}, P_{Tb} > 30 \text{ GeV}$	0.1008	3593.325	5.0506	10.684	144.19	1.169	0.01	$2.7 \times 10^{-6}$
$\Delta R_{\ell\ell} < 1.0, \Delta R_{bb} < 1.0$	0.015	30.59	0.065	0.175	0.9424	0.0254	0.146	$4.7 \times 10^{-4}$
$m_{\ell\ell} < 65 \text{ GeV}, 95 \text{ GeV} < m_{bb} < 140 \text{ GeV}$	0.00784	0.4746	0.0165	0.01287	0.0228	0.0039	0.58	0.0148
$\cancel{E}_T > 50 \text{ GeV}$	0.00682	0.4	0.0144	0.0116	0.023	0.0039	0.553	0.015
$\cancel{E}_T > 80 \text{ GeV}$	0.0058	0.268	0.01	0.0099	0.0228	0.0039	0.564	0.018
$\cancel{E}_T > 120 \text{ GeV}$	0.00433	0.0603	0.006	0.0064	0.0114	0.0039	0.793	0.049

- Proximity cut of  $\Delta R_{\ell\ell} < 1.0$  for the two leptons;
- Proximity cut of  $\Delta R_{bb} < 1.0$  for two  $b$ -tagged jets;
- $m_{\ell\ell} < 65 \text{ GeV}$  for two leptons;
- $95 \text{ GeV} < m_{bb} < 140 \text{ GeV}$  for the two  $b$ -tagged jets;
- $\cancel{E}_T = |\vec{\cancel{p}}_T| > 120 \text{ GeV}$  for the reconstructed missing transverse momentum.

From our simulation result, we find the  $b\bar{b}\tau\tau$  background can be greatly suppressed, while the  $t\bar{t}$  background remains to be the dominant one. Finally the significance can only reach  $0.79 \sigma$ . Although we can increase the value of  $\mu$  to relatively enhance the signal events with  $\cancel{E}_T > 120 \text{ GeV}$ , this will also suppress the total signal cross section and thus cannot enhance the significance. So we conclude that this channel cannot be observed at the HL-LHC.

### 3.2 The signal of $hhG'G' \rightarrow b\bar{b}b\bar{b} + \cancel{E}_T$

Now we turn to the decay channel  $hhG'G' \rightarrow b\bar{b}b\bar{b} + \cancel{E}_T$ . The decay  $h \rightarrow b\bar{b}$  has the largest branching ratio of 58%. In the SM this channel from the Higgs pair production suffers from overwhelming QCD multi-jet backgrounds and its significance can only reach  $1.8\sigma$  at the HL-LHC [69]. In our scenario, we have large missing energy which helps to suppress the QCD multi-jet backgrounds. Considering the missing energy, the backgrounds for the signal  $b\bar{b}b\bar{b} + \cancel{E}_T$  are the QCD multi-jets plus  $W$  or  $Z$  boson.

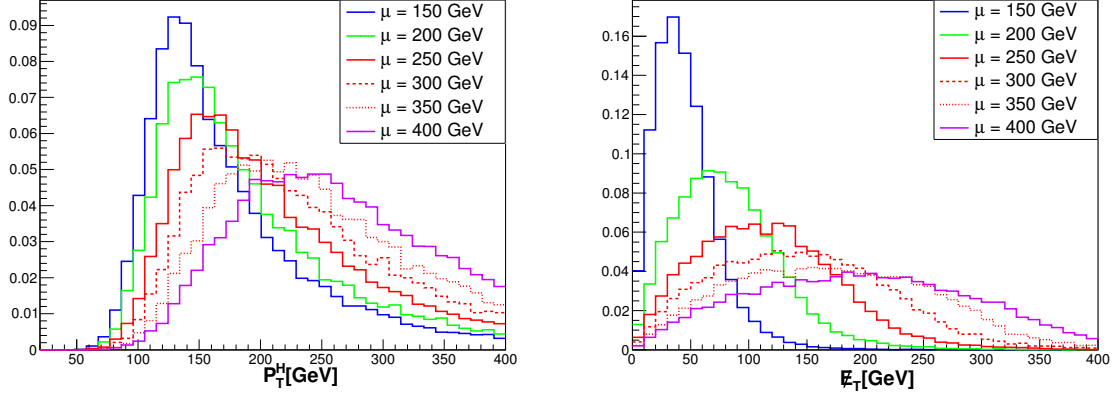


**Figure 4.** Distributions of  $P_T$  of the leading Higgs and  $E_T$  for the signal  $bb\bar{b}\bar{b} + E_T$  with different values of  $\mu$ . The  $y$ -axis represents the normalized number of events.

In the case of multi-jets plus a  $W$  boson, it can fake the signal when the  $W$  boson decays to  $\ell\nu$  with the charged lepton missing detection (too soft, travelling along the beamline or too close to a jet) or the  $W$  boson decaying to  $\tau\nu$  with the secondary jet from the hadronic  $\tau$  decay missing detection. For the case of multi-jets plus a  $Z$  boson, it can fake the signal when  $Z$  decays to  $\nu\bar{\nu}$ . Although their cross sections are about 1-2 pb, much larger than the cross section of the signal, they are not the major backgrounds due to the small fake efficiency. The  $t\bar{t}h(h \rightarrow b\bar{b})$  process, which was not the main background in the preceding section, is now likely the major background. So we consider the backgrounds from  $bbbbZ$ ,  $bbjjW^\pm(W^\pm \rightarrow \ell\nu)$ ,  $bbjjW^\pm(W^\pm \rightarrow \tau\nu)$ ,  $bbjjZ$  and  $t\bar{t}h(h \rightarrow b\bar{b})$  processes. All these backgrounds are generated using MadGraph with the PDF CTEQ6L1 [70] at the leading order. Since the cross-section of this signal is large enough even for a relatively large  $\mu$ , we will choose different values of  $\mu$  to show the results. At the parton level, we simply require  $p_{Tj} > 30$  GeV,  $|\eta_j| < 2.7$ ,  $\Delta R_{jj} > 0.4$  in our simulations.

We note that the triggers and jet reconstructions are very important for the signal, in which the transverse momentum of the Higgs boson plays a key role. So after parton-shower and hadronization, we show the  $P_T$  of the leading Higgs and  $E_T$  distributions in Fig. 4. We find that the signal has relatively low transverse momentum for the Higgs, which is typically below 200 GeV for the value of  $\mu$  below 400 GeV. We require at least four anti- $k_t$   $R=0.4$   $b$ -jets for the signal (the efficiency for reconstructing a Higgs boson from two anti- $k_t$   $R=0.4$  jets is higher than reconstructing from a Cambridge-Aachen jet with  $R=1.2$  in this case [69]).

So the four  $b$ -tagged jets are required, paired into two dijets, to reconstruct the

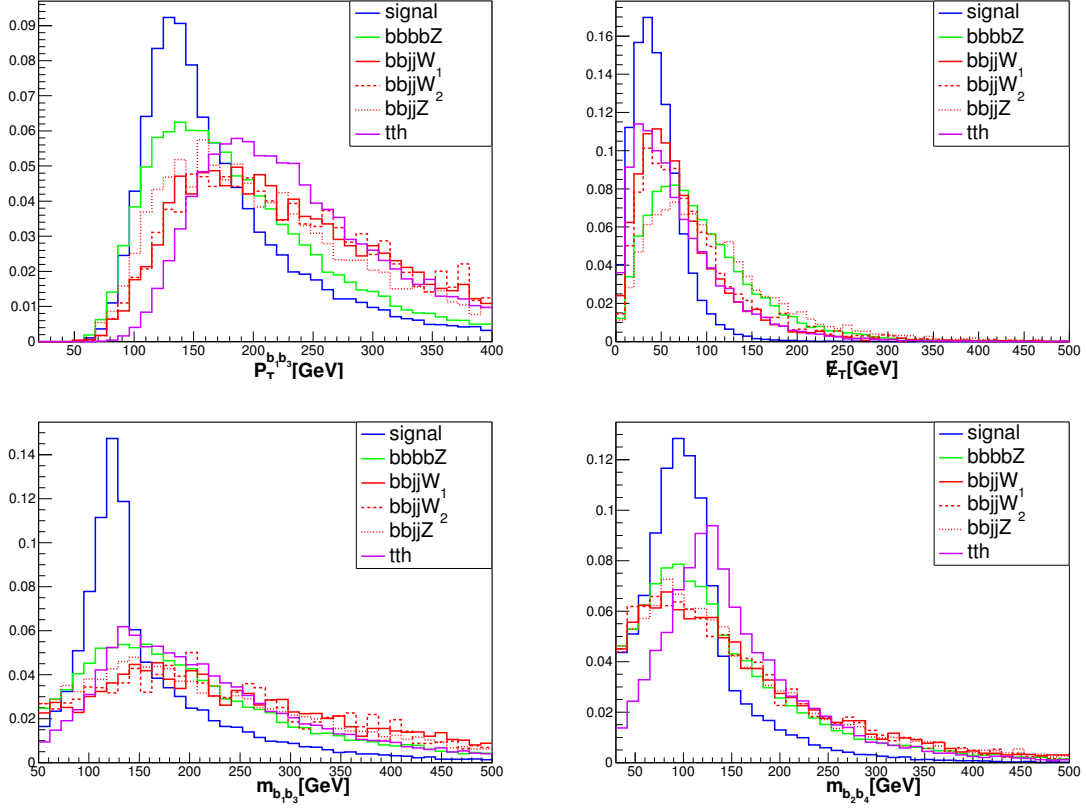


**Figure 5.** Distributions of signal and backgrounds after basic cuts for  $\mu = 150$  GeV. The  $y$ -axis represents the normalized number of events

Higgs bosons, and this is a powerful way to reduce the backgrounds. Firstly, we rank the  $b$ -jets from largest to smallest according to their  $P_T$ . Then there are three ways to pair the four  $b$ -jets and from the reconstructing efficiencies we get to know the correct way, with  $b_1 b_3$  for a Higgs and  $b_2 b_4$  for the other finally.

After detector simulation, we display the distributions in Fig. 5 for  $\mu = 150$  GeV. From the distributions we can find the distributions of  $P_T^{b_1} + P_T^{b_3} \equiv P_T^{b_1 b_3}$  and  $P_T^{b_2} + P_T^{b_4} \equiv P_T^{b_2 b_4}$  can be used to effectively suppress the background of  $t\bar{t}h$ . So we apply cuts  $90 \text{ GeV} < P_T^{b_1 b_3} < 190 \text{ GeV}$  and  $80 \text{ GeV} < P_T^{b_2 b_4} < 180 \text{ GeV}$  for the four  $b$ -tagged jets. With these cuts, the significance can reach  $18.7\sigma$ , as shown in Table 2.

As  $\mu$  increases, the signal cross-section decreases rapidly, but its missing energy and  $P_T^H$  also increase, as shown in Fig. 4. We take  $\mu = 350$  GeV as an example to show the analysis. We use  $P_T^{b_1 b_3}$  and  $P_T^{b_2 b_4}$  to suppress the multi-jet backgrounds by requiring  $P_T^{b_1 b_3} > 100 \text{ GeV}$  and  $P_T^{b_2 b_4} > 160 \text{ GeV}$ . Since the angular separations have no

**Table 2.** Signal and background cross sections in fb after the cuts for  $\mu = 150$  GeV. The significance  $\sigma$  is calculated for a luminosity of  $3 \text{ ab}^{-1}$  at the 14 TeV LHC.

Cuts	signal	bbbbZ	bbjjW <sub>1</sub>	bbjjW <sub>2</sub>	bbjjZ	tth(bb)	$\sigma$	S/B
$190 \text{ GeV} > P_T^{b_1 b_3} > 90 \text{ GeV}, 180 \text{ GeV} > P_T^{b_2 b_4} > 80 \text{ GeV}$	0.618	0.209	0.409	0.219	0.582	1.636	18.7	2.02

**Table 3.** Signal and background cross sections in fb after cuts at different stages for  $\mu = 350$  GeV.

Cuts	signal	bbbbZ	bbjjW <sub>1</sub>	bbjjW <sub>2</sub>	bbjjZ	tth(bb)	$\sigma$	S/B
$P_T^{b_1 b_3} > 100 \text{ GeV}, P_T^{b_2 b_4} > 160 \text{ GeV}$	0.072	0.276	1.205	0.619	1.241	4.925	1.34	0.008
$0.4 < \Delta R_{b_1 b_3} < 3.5, 0.4 < \Delta R_{b_2 b_4} < 3$	0.057	0.175	0.742	0.379	0.752	3.871	1.33	0.0085
$90 \text{ GeV} < m_{b_1 b_3} < 140 \text{ GeV}, 85 \text{ GeV} < m_{b_2 b_4} < 130 \text{ GeV}$	0.014	0.0067	0.0182	0.0073	0.02	0.215	1.49	0.0077
$\cancel{E}_T > 150 \text{ GeV}$	0.0086	0.0013	0.0023	0.0005	0.0057	0.0178	2.74	0.311

obvious difference between signal and backgrounds, we set loose cuts  $0.4 < \Delta R_{b_1 b_3} < 3$  and  $0.4 < \Delta R_{b_2 b_4} < 3.5$ . Furthermore, since the invariant mass cuts have suppression on all backgrounds except  $t\bar{t}h$ , we set cuts  $90 \text{ GeV} < m_{b_1 b_3} < 145 \text{ GeV}$  and  $80 \text{ GeV} < m_{b_2 b_4} < 140 \text{ GeV}$ .  $\cancel{E}_T$  can suppress all backgrounds in this case and we set  $\cancel{E}_T > 150 \text{ GeV}$ . The detailed results are shown in Table 3.

From the above results we find that the  $\cancel{E}_T$  cut plays a major role in distinguishing the signal from the backgrounds for a large  $\mu$ . The detailed cuts are summarized as follows:

- The four leading jets must be  $b$ -tagged;
- Exactly two Higgs are reconstructed, with  $p_T^{b_1 b_3} > 100 \text{ GeV}$  and  $p_T^{b_2 b_4} > 160 \text{ GeV}$ ;
- Proximity cut of  $0.4 < \Delta R_{b_1 b_3} < 3$  for one Higgs, and  $0.4 < \Delta R_{b_2 b_4} < 3.5$  for the other;
- $90 \text{ GeV} < m_{b_1 b_3} < 140 \text{ GeV}$  and  $85 \text{ GeV} < m_{b_2 b_4} < 130 \text{ GeV}$  for the  $b$ -tagged jets;
- $\cancel{E}_T > 150 \text{ GeV}$  for the reconstructed missing transverse momentum.

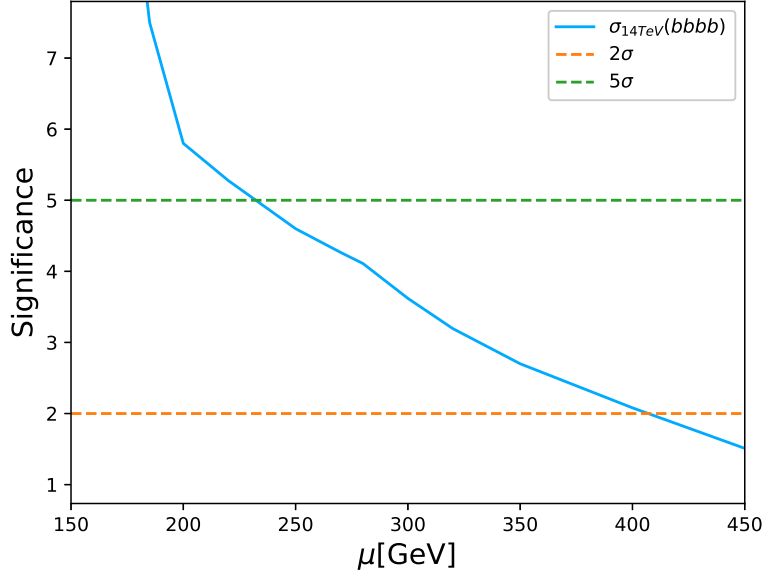


**Figure 6.** The signal  $bbbb + \cancel{E}_T$  significance versus the  $\mu$  value at the HL-LHC ( $3 \text{ ab}^{-1}$ , 14 TeV).

After the sequential cuts, we find that the multi-jets background are greatly suppressed, while the  $t\bar{t}h$  background remains large and will be further cut with a larger  $\cancel{E}_T$ . With the increase of  $\mu$  value, the signal cross-section will be reduced but the cut with a larger  $\cancel{E}_T$  can help for the signal significance. For  $\mu = 350$  GeV, the signal significance can reach to  $2.74\sigma$ , as shown in Fig. 6. As  $\mu$  increases above 400 GeV the significance drops below  $2\sigma$ . Note that in this scenario the  $\mu$  value determines the lightest neutralino mass.

### 3.3 The signal of $hhG'G' \rightarrow b\bar{b}\gamma\gamma + \cancel{E}_T$

Finally we turn to the third channel with  $h \rightarrow b\bar{b}$  and  $h \rightarrow \gamma\gamma$ . It has a pair of photons reconstructed at the invariant mass around the Higgs boson. So the backgrounds include the single Higgs production such as  $t\bar{t}H$ . For non-resonant backgrounds and jet-fake backgrounds, we should consider missing energy based on the backgrounds considered in the preceding section. From the calculation we mainly need to consider the backgrounds from  $bbj\gamma W^\pm (W^\pm \rightarrow \ell^\pm \nu)$ ,  $bbj\gamma W^\pm (W^\pm \rightarrow \tau^\pm \nu)$ ,  $bbj\gamma Z (Z \rightarrow \nu\bar{\nu})$ ,  $bbbbZ$ , and  $t\bar{t}\gamma$  productions.

The parton-level events for backgrounds are generated with MadGraph5, using the

PDF CTEQ6L1 [70]. For the signal calculation, it involves the loop-induced Higgs decay to di-photon and we use the loop-induced model [71]. The parton-level cuts are imposed in order to avoid any divergence in the parton-level calculation [72]:  $P_{Tj} > 20$  GeV,  $P_{T\gamma} > 25$  GeV,  $|\eta_j| < 2.5$ ,  $|\eta_\gamma| < 2.5$ ,  $m_{jj} > 25$  GeV.

For signal and backgrounds we require a pair of isolated photons and a pair of isolated  $b$ -tagged jets which are reconstructed near the Higgs boson mass. In Fig. 7, we show the distributions of  $P_T^{bb}$ ,  $P_T^{\gamma\gamma}$ ,  $\cancel{E}_T$ ,  $m_{\gamma\gamma}$  and  $m_{bb}$  for signal and backgrounds. Since the angular separations have no obvious difference between signal and backgrounds, we set loose cuts  $1.0 < \Delta R_{bb} < 3.8$  and  $1 < \Delta R_{\gamma\gamma} < 3.7$ . Obviously,  $m_{\gamma\gamma}$  and  $P_T^{\gamma\gamma}$  have distinctive features to distinguish signal from backgrounds except  $t\bar{t}h$ . In order to reduce the background of  $t\bar{t}h$ , we require  $P_T^{bb}$  in the range of  $[80, 250]$  GeV and  $P_T^{\gamma\gamma} > 70$  GeV. The  $\cancel{E}_T$  cut can efficiently suppress the multi-jet backgrounds and we set  $10 \text{ GeV} < \cancel{E}_T < 90 \text{ GeV}$ . The cuts can be summarized in the following:

- The two leading jets must be  $b$ -tagged with  $250 \text{ GeV} > p_T^{bb} > 80 \text{ GeV}$ ;
- Exactly two isolated photons with  $p_T^{\gamma\gamma} > 70 \text{ GeV}$ ;
- Proximity cut of  $1 < \Delta R_{\gamma\gamma} < 3.7$  for the two photons;
- Proximity cut of  $1 < \Delta R_{bb} < 3.8$  for the two  $b$ -tagged jets;
- $121 \text{ GeV} < m_{\gamma\gamma} < 128 \text{ GeV}$  for the two photons;
- $100 \text{ GeV} < m_{bb} < 250 \text{ GeV}$  for the two  $b$ -tagged jets;
- $90 \text{ GeV} > \cancel{E}_T = |\vec{\cancel{P}}_T| > 10 \text{ GeV}$  for the reconstructed missing transverse momentum.

The detailed results are shown in Table 4. From our analysis we find that the  $t\bar{t}\gamma$  background still remains large after these cuts. The signal significance can only reach to  $1\sigma$ .

Some remarks are in order. From our results we know that for the three channels only the  $bbbb + \cancel{E}_T$  signal is observable at the HL-LHC. In our studies we used the traditional cut-flow Monte Carlo simulations. Note that some machine learning methods (for a review, see, e.g., [73]) may help to enhance the signal significance, e.g., the graph neural network was found to significantly enhance the top-squark and Higgs pair signal significances at the LHC [74, 75]. In addition, we did not consider the explanation of the muon  $g-2$  in our scenario, which was found (see, e.g., [76–79]) to require light neutralinos/charginos and light sleptons, possibly accessible at the HL-LHC [76]. For the status of low-energy supersymmetry confronted with current experimental constraints,

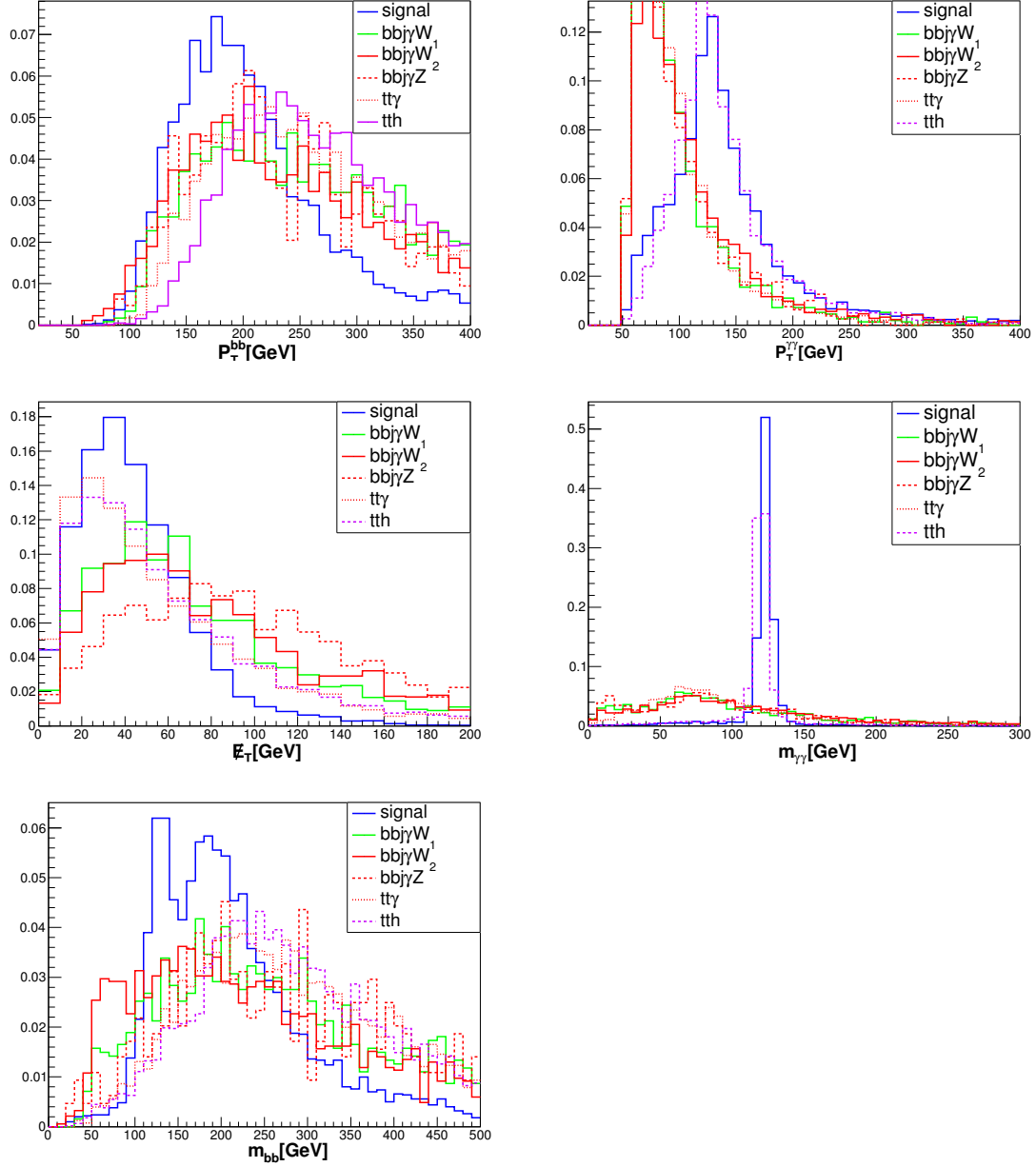


**Figure 7.** Distributions for the signal with  $\mu = 150$  GeV and backgrounds. The  $y$ -axis represents the normalized number of events for each process.

such as collider searches, dark matter searches and muon  $g - 2$  measurement, recent overviews could be found in Refs. [80, 81].

Finally, we point out that our study may be also applicable to higgsino decay into

**Table 4.** The cut flow for signal and background cross sections in fb for a luminosity of  $3 \text{ ab}^{-1}$  at the 14 TeV LHC.

Cuts	signal	$b\bar{b}j\gamma W_1$	$b\bar{b}j\gamma W_2$	$b\bar{b}jZ$	$t\bar{t}\gamma$	$t\bar{t}h$	$\sigma$	$S/B$
$80 \text{ GeV} < P_T^{bb} < 250 \text{ GeV}, P_T^{\gamma\gamma} > 70 \text{ GeV}$	0.0093	0.0466	0.036	0.044	4.09	0.011	0.25	0.0022
$100 \text{ GeV} < m_{bb} < 250 \text{ GeV}, 121 < m_{\gamma\gamma} < 128 \text{ GeV}$	0.0051	0.0008	0.001	0.0005	0.089	0.0026	0.9	0.054
$90 \text{ GeV} > \cancel{E}_T > 10 \text{ GeV}$	0.0047	0.0006	0.0009	0	0.067	0.0021	1	0.072

a light singlino (which can be rather light as the lightest superparticle [82]) plus a Higgs boson in the NMSSM which introduces a singlet Higgs superfield, mixing with the Higgs doublets, and thus relieves the 125 GeV Higgs mass constraint on stop masses [83].

## 4 Conclusion

We considered the scenario of multi-sector SUSY breaking which predicts light pseudo-goldstinos and opens the decay mode of higgsino into pseudo-goldstino plus Higgs boson inside the detector at the LHC, leading to the signal of Higgs pair plus missing energy. We studied the observability of such Higgs pair plus missing energy from the decay of higgsinos produced at the HL-LHC (14 TeV with a luminosity of  $3 \text{ ab}^{-1}$ ). We considered light higgsinos assumed in natural SUSY and studied the three decay channels of the Higgs pair ( $b\bar{b}WW^*$ ,  $b\bar{b}\gamma\gamma$ ,  $b\bar{b}b\bar{b}$ ). From detailed Monte Carlo simulations for the signal and backgrounds, the following observations are obtained: (i) The best channel is  $b\bar{b}b\bar{b} + \cancel{E}_T$ , whose statistical significance can reach  $5\sigma$  for a light higgsino in natural SUSY allowed by current experiments; (ii) The channels  $b\bar{b}\gamma\gamma + \cancel{E}_T$  and  $b\bar{b}WW^* + \cancel{E}_T$  respectively give maximal statistical significance of  $1\sigma$  and  $0.79\sigma$ . So the Higgs pair plus missing energy signal from the higgsino decay can be significantly over the SM Higgs pair result which is about  $1.8\sigma$  at the HL-LHC.

## Acknowledgments

This work was supported in part by IHEP under Grant No. Y9515570U1, by the National Natural Science Foundation of China (NNSFC) under grant Nos. 11821505 and 12075300, by Peng-Huan-Wu Theoretical Physics Innovation Center (12047503), by the CAS Center for Excellence in Particle Physics (CCEPP), by the CAS Key



Research Program of Frontier Sciences, and by a Key R&D Program of Ministry of Science and Technology of China under number 2017YFA0402204, and by the Key Research Program of the Chinese Academy of Sciences, Grant NO. XDPB15.

## Note added:

When preparing this manuscript, the CMS collaboration reported their search results for the signal of Higgs pair plus missing energy using an integrated luminosity of  $137 \text{ fb}^{-1}$  [84]. When applied to higgsino decay into Higgs plus pseudo-goldstino, a range  $305 \text{ GeV} > m_{\tilde{\chi}_1^0} (\simeq \mu) > 265 \text{ GeV}$  can be excluded by this CMS search, assuming the decay branching ratio to be 1. Since in our study we assumed the branching ratio of higgsino decay to Higgs plus pseudo-goldstino to be 0.5, this excluded range  $305 \text{ GeV} > m_{\tilde{\chi}_1^0} (\simeq \mu) > 265 \text{ GeV}$  will become much narrower when applied to our scenario.

## References

- [1] ATLAS collaboration, M. Aaboud et al., *Search for Higgs boson pair production in the  $b\bar{b}WW^*$  decay mode at  $\sqrt{s} = 13 \text{ TeV}$  with the ATLAS detector*, [1811.04671](#).
- [2] CMS collaboration, *Search for resonant and non-resonant Higgs boson pair production in the  $b\bar{b}l\nu l\nu$  final state at  $\sqrt{s} = 13 \text{ TeV}$* , [CMS-PAS-HIG-17-006](#).
- [3] ATLAS collaboration, M. Aaboud et al., *Search for pair production of Higgs bosons in the  $b\bar{b}b\bar{b}$  final state using proton-proton collisions at  $\sqrt{s} = 13 \text{ TeV}$  with the ATLAS detector*, *JHEP* **01** (2019) 030, [[1804.06174](#)].
- [4] CMS collaboration, *Search for Non-Resonant Higgs Pair-Production in the  $b\bar{b}b\bar{b}$  Final State with the CMS detector*, [CMS-PAS-HIG-17-017](#).
- [5] CMS collaboration, A. M. Sirunyan et al., *Search for Higgs boson pair production in the  $\gamma\gamma b\bar{b}$  final state in  $pp$  collisions at  $\sqrt{s} = 13 \text{ TeV}$* , *Phys. Lett.* **B788** (2019) 7–36, [[1806.00408](#)].
- [6] ATLAS collaboration, M. Aaboud et al., *Search for Higgs boson pair production in the  $\gamma\gamma b\bar{b}$  final state with 13 TeV  $pp$  collision data collected by the ATLAS experiment*, *JHEP* **11** (2018) 040, [[1807.04873](#)].
- [7] ATLAS collaboration, M. Aaboud et al., *Search for resonant and non-resonant Higgs boson pair production in the  $b\bar{b}\tau^+\tau^-$  decay channel in  $pp$  collisions at  $\sqrt{s} = 13 \text{ TeV}$  with the ATLAS detector*, *Phys. Rev. Lett.* **121** (2018) 191801, [[1808.00336](#)].
- [8] CMS collaboration, A. M. Sirunyan et al., *Search for Higgs boson pair production in events with two bottom quarks and two tau leptons in proton-proton collisions at  $\sqrt{s} = 13 \text{ TeV}$* , *Phys. Lett.* **B778** (2018) 101–127, [[1707.02909](#)].

- [9] ATLAS collaboration, M. Aaboud et al., *Search for Higgs boson pair production in the  $WW^{(*)}WW^{(*)}$  decay channel using ATLAS data recorded at  $\sqrt{s} = 13$  TeV*, [1811.11028](#).
- [10] G. Aad, B. Abbott, D. Abbott, A. Abed Abud, K. Abeling, D. Abhayasinghe et al., *Combination of searches for higgs boson pairs in pp collisions at  $\sqrt{s} = 13$  tev with the atlas detector*, *Physics Letters B* **800** (Jan, 2020) 135103.
- [11] R. Contino, C. Grojean, M. Moretti, F. Piccinini and R. Rattazzi, *Strong Double Higgs Production at the LHC*, *JHEP* **05** (2010) 089, [[1002.1011](#)].
- [12] R. Grober and M. Muhlleitner, *Composite Higgs Boson Pair Production at the LHC*, *JHEP* **06** (2011) 020, [[1012.1562](#)].
- [13] M. J. Dolan, C. Englert and M. Spannowsky, *New Physics in LHC Higgs boson pair production*, *Phys. Rev. D* **87** (2013) 055002, [[1210.8166](#)].
- [14] C. Han, X. Ji, L. Wu, P. Wu and J. M. Yang, *Higgs pair production with SUSY QCD correction: revisited under current experimental constraints*, *JHEP* **04** (2014) 003, [[1307.3790](#)].
- [15] B. Hespel, D. Lopez-Val and E. Vryonidou, *Higgs pair production via gluon fusion in the Two-Higgs-Doublet Model*, *JHEP* **09** (2014) 124, [[1407.0281](#)].
- [16] J. Cao, D. Li, L. Shang, P. Wu and Y. Zhang, *Exploring the Higgs Sector of a Most Natural NMSSM and its Prediction on Higgs Pair Production at the LHC*, *JHEP* **12** (2014) 026, [[1409.8431](#)].
- [17] S. Dawson, A. Ismail and I. Low, *What's in the loop? The anatomy of double Higgs production*, *Phys. Rev. D* **91** (2015) 115008, [[1504.05596](#)].
- [18] L.-C. Lü, C. Du, Y. Fang, H.-J. He and H. Zhang, *Searching heavier Higgs boson via di-Higgs production at LHC Run-2*, *Phys. Lett. B* **755** (2016) 509–522, [[1507.02644](#)].
- [19] Z. Kang, P. Ko and J. Li, *New Physics Opportunities in the Boosted Di-Higgs-Boson Plus Missing Transverse Energy Signature*, *Phys. Rev. Lett.* **116** (2016) 131801, [[1504.04128](#)].
- [20] K. Nakamura, K. Nishiwaki, K.-y. Oda, S. C. Park and Y. Yamamoto, *Di-higgs enhancement by neutral scalar as probe of new colored sector*, *Eur. Phys. J. C* **77** (2017) 273, [[1701.06137](#)].
- [21] J. Chang, C.-R. Chen and C.-W. Chiang, *Higgs boson pair productions in the Georgi-Machacek model at the LHC*, *JHEP* **03** (2017) 137, [[1701.06291](#)].
- [22] J. Ren, R.-Q. Xiao, M. Zhou, Y. Fang, H.-J. He and W. Yao, *LHC Search of New Higgs Boson via Resonant Di-Higgs Production with Decays into  $4W$* , *JHEP* **06** (2018) 090, [[1706.05980](#)].
- [23] P. Huang, A. Joglekar, M. Li and C. E. M. Wagner, *Corrections to di-Higgs boson*

- production with light stops and modified Higgs couplings*, *Phys. Rev. D* **97** (2018) 075001, [[1711.05743](#)].
- [24] A. Adhikary, S. Banerjee, R. K. Barman, B. Bhattacharjee and S. Niyogi, *Revisiting the non-resonant Higgs pair production at the HL-LHC*, *JHEP* **07** (2018) 116, [[1712.05346](#)].
  - [25] P. Agrawal, D. Saha, L.-X. Xu, J.-H. Yu and C. P. Yuan, *Determining the shape of the Higgs potential at future colliders*, *Phys. Rev. D* **101** (2020) 075023, [[1907.02078](#)].
  - [26] K. Cheung, A. Jueid, C.-T. Lu, J. Song and Y. W. Yoon, *Disentangling new physics effects on nonresonant Higgs boson pair production from gluon fusion*, *Phys. Rev. D* **103** (2021) 015019, [[2003.11043](#)].
  - [27] H. Abouabid, A. Arhrib, D. Azevedo, J. E. Falaki, P. M. Ferreira, M. Mühlleitner et al., *Benchmarking Di-Higgs Production in Various Extended Higgs Sector Models*, [2112.12515](#).
  - [28] L. Wu, J. M. Yang, C.-P. Yuan and M. Zhang, *Higgs self-coupling in the MSSM and NMSSM after the LHC Run 1*, *Phys. Lett. B* **747** (2015) 378–389, [[1504.06932](#)].
  - [29] L. Wang, W. Wang, J. M. Yang and H. Zhang, *Higgs-pair production in littlest Higgs model with  $T$ -parity*, *Phys. Rev. D* **76** (2007) 017702, [[0705.3392](#)].
  - [30] X.-F. Han, L. Wang and J. M. Yang, *Higgs-pair Production and Decay in Simplest Little Higgs Model*, *Nucl. Phys. B* **825** (2010) 222–230, [[0908.1827](#)].
  - [31] R. Argurio, Z. Komargodski and A. Mariotti, *Pseudo-Goldstini in Field Theory*, *Phys. Rev. Lett.* **107** (2011) 061601, [[1102.2386](#)].
  - [32] J. Dai, T. Liu and J. M. Yang, *An explicit calculation of pseudo-goldstino mass at the leading three-loop level*, *JHEP* **06** (2021) 175, [[2104.12656](#)].
  - [33] C. Cheung, Y. Nomura and J. Thaler, *Goldstini*, *JHEP* **03** (2010) 073, [[1002.1967](#)].
  - [34] C. Cheung, J. Mardon, Y. Nomura and J. Thaler, *A Definitive Signal of Multiple Supersymmetry Breaking*, *JHEP* **07** (2010) 035, [[1004.4637](#)].
  - [35] N. Craig, J. March-Russell and M. McCullough, *The Goldstini Variations*, *JHEP* **10** (2010) 095, [[1007.1239](#)].
  - [36] J. Thaler and Z. Thomas, *Goldstini Can Give the Higgs a Boost*, *JHEP* **07** (2011) 060, [[1103.1631](#)].
  - [37] C. Cheung, F. D’Eramo and J. Thaler, *The Spectrum of Goldstini and Modulini*, *JHEP* **08** (2011) 115, [[1104.2600](#)].
  - [38] R. Argurio, K. De Causmaecker, G. Ferretti, A. Mariotti, K. Mawatari and Y. Takaesu, *Collider signatures of goldstini in gauge mediation*, *JHEP* **06** (2012) 096, [[1112.5058](#)].
  - [39] E. Dudas, G. von Gersdorff, D. M. Ghilencea, S. Lavignac and J. Parmentier, *On*

- non-universal Goldstino couplings to matter*, *Nucl. Phys. B* **855** (2012) 570–591, [[1106.5792](#)].
- [40] T. Liu, L. Wang and J. M. Yang, *Higgs decay to goldstini and its observability at the LHC*, *Phys. Lett. B* **726** (2013) 228–233, [[1301.5479](#)].
  - [41] K.-i. Hikasa, T. Liu, L. Wang and J. M. Yang, *Pseudo-goldstino and electroweak gauginos at the LHC*, *JHEP* **07** (2014) 065, [[1403.5731](#)].
  - [42] T. Liu, L. Wang and J. M. Yang, *Pseudo-goldstino and electroweakinos via VBF processes at LHC*, *JHEP* **02** (2015) 177, [[1411.6105](#)].
  - [43] G. Ferretti, A. Mariotti, K. Mawatari and C. Petersson, *Multiphoton signatures of goldstini at the LHC*, *JHEP* **04** (2014) 126, [[1312.1698](#)].
  - [44] D. B. Franzosi, G. Ferretti, E. Riefel and S. Strandberg, *Electroweak signatures of gauge-mediated supersymmetry breaking in multiple hidden sectors*, *JHEP* **01** (2022) 139, [[2111.04775](#)].
  - [45] C. Brust, A. Katz, S. Lawrence and R. Sundrum, *SUSY, the Third Generation and the LHC*, *JHEP* **03** (2012) 103, [[1110.6670](#)].
  - [46] M. Papucci, J. T. Ruderman and A. Weiler, *Natural SUSY Endures*, *JHEP* **09** (2012) 035, [[1110.6926](#)].
  - [47] L. J. Hall, D. Pinner and J. T. Ruderman, *A Natural SUSY Higgs Near 126 GeV*, *JHEP* **04** (2012) 131, [[1112.2703](#)].
  - [48] J. L. Feng and D. Sanford, *A Natural 125 GeV Higgs Boson in the MSSM from Focus Point Supersymmetry with A-Terms*, *Phys. Rev. D* **86** (2012) 055015, [[1205.2372](#)].
  - [49] H. Baer, V. Barger, P. Huang, A. Mustafayev and X. Tata, *Radiative natural SUSY with a 125 GeV Higgs boson*, *Phys. Rev. Lett.* **109** (2012) 161802, [[1207.3343](#)].
  - [50] X. Tata, *Natural supersymmetry: status and prospects*, *Eur. Phys. J. ST* **229** (2020) 3061–3083, [[2002.04429](#)].
  - [51] C. Han, A. Kobakhidze, N. Liu, A. Saavedra, L. Wu and J. M. Yang, *Probing Light Higgsinos in Natural SUSY from Monojet Signals at the LHC*, *JHEP* **02** (2014) 049, [[1310.4274](#)].
  - [52] GAMBIT collaboration, P. Athron et al., *Combined collider constraints on neutralinos and charginos*, *Eur. Phys. J. C* **79** (2019) 395, [[1809.02097](#)].
  - [53] B. Allanach, *Softsusy: A program for calculating supersymmetric spectra*, *Computer Physics Communications* **143** (Mar, 2002) 305–331.
  - [54] J. Grigo, K. Melnikov and M. Steinhauser, *Virtual corrections to Higgs boson pair production in the large top quark mass limit*, *Nucl. Phys. B* **888** (2014) 17–29, [[1408.2422](#)].

- [55] J. Alwall, R. Frederix, S. Frixione, V. Hirschi, F. Maltoni, O. Mattelaer et al., *The automated computation of tree-level and next-to-leading order differential cross sections, and their matching to parton shower simulations*, *JHEP* **07** (2014) 079, [[1405.0301](#)].
- [56] NNPDF collaboration, R. D. Ball, V. Bertone, S. Carrazza, L. Del Debbio, S. Forte, A. Guffanti et al., *Parton distributions with QED corrections*, *Nucl. Phys.* **B877** (2013) 290–320, [[1308.0598](#)].
- [57] W. Beenakker, M. Klasen, M. Kramer, T. Plehn, M. Spira and P. M. Zerwas, *The Production of charginos / neutralinos and sleptons at hadron colliders*, *Phys. Rev. Lett.* **83** (1999) 3780–3783, [[hep-ph/9906298](#)].
- [58] A. Alloul, N. D. Christensen, C. Degrande, C. Duhr and B. Fuks, *Feynrules 2.0 — a complete toolbox for tree-level phenomenology*, *Computer Physics Communications* **185** (Aug, 2014) 2250–2300.
- [59] C. Degrande, C. Duhr, B. Fuks, D. Grellscheid, O. Mattelaer and T. Reiter, *Ufo – the universal feynrules output*, *Computer Physics Communications* **183** (Jun, 2012) 1201–1214.
- [60] T. Sjostrand, S. Ask, J. R. Christiansen, R. Corke, N. Desai, P. Ilten et al., *An Introduction to PYTHIA 8.2*, *Comput. Phys. Commun.* **191** (2015) 159–177, [[1410.3012](#)].
- [61] DELPHES 3 collaboration, J. de Favereau, C. Delaere, P. Demin, A. Giammanco, V. Lemaitre, A. Mertens et al., *DELPHES 3, A modular framework for fast simulation of a generic collider experiment*, *JHEP* **02** (2014) 057, [[1307.6346](#)].
- [62] M. Cacciari, G. P. Salam and G. Soyez, *FastJet User Manual*, *Eur. Phys. J.* **C72** (2012) 1896, [[1111.6097](#)].
- [63] M. Cacciari, G. P. Salam and G. Soyez, *The anti- $k_t$  jet clustering algorithm*, *JHEP* **04** (2008) 063, [[0802.1189](#)].
- [64] ATLAS collaboration, *Expected performance of the ATLAS detector at the High-Luminosity LHC*, Tech. Rep. ATL-PHYS-PUB-2019-005, CERN, Geneva, Jan, 2019.
- [65] J. H. Kim, M. Kim, K. Kong, K. T. Matchev and M. Park, *Portraying double higgs at the large hadron collider*, *Journal of High Energy Physics* **2019** (Sep, 2019) .
- [66] M. Czakon, P. Fiedler and A. Mitov, *Total Top-Quark Pair-Production Cross Section at Hadron Colliders Through  $\mathcal{O}(\alpha_S^4)$* , *Phys. Rev. Lett.* **110** (2013) 252004, [[1303.6254](#)].
- [67] LHC HIGGS CROSS SECTION WORKING GROUP collaboration, S. Dittmaier et al., *Handbook of LHC Higgs Cross Sections: 1. Inclusive Observables*, [1101.0593](#).
- [68] LHC HIGGS CROSS SECTION WORKING GROUP collaboration, D. de Florian et al.,

*Handbook of LHC Higgs Cross Sections: 4. Deciphering the Nature of the Higgs Sector*, [1610.07922](#).

- [69] D. Wardrope, E. Jansen, N. Konstantinidis, B. Cooper, R. Falla and N. Norjoharuddeen, *Non-resonant higgs-pair production in the  $b\bar{b}b\bar{b}$  final state at the lhc*, *The European Physical Journal C* **75** (May, 2015) .
- [70] D. Stump, J. Huston, J. Pumplin, W.-K. Tung, H.-L. Lai, S. Kuhlmann et al., *Inclusive jet production, parton distributions, and the search for new physics*, *Journal of High Energy Physics* **2003** (Oct, 2003) 046–046.
- [71] V. Hirschi and O. Mattelaer, *Automated event generation for loop-induced processes*, *JHEP* **10** (2015) 146, [[1507.00020](#)].
- [72] ATLAS collaboration, *Study of the double Higgs production channel  $H(\rightarrow b\bar{b})H(\rightarrow \gamma\gamma)$  with the ATLAS experiment at the HL-LHC*, .
- [73] M. Abdughani, J. Ren, L. Wu, J. M. Yang and J. Zhao, *Supervised deep learning in high energy phenomenology: a mini review*, *Commun. Theor. Phys.* **71** (2019) 955, [[1905.06047](#)].
- [74] M. Abdughani, J. Ren, L. Wu and J. M. Yang, *Probing stop pair production at the LHC with graph neural networks*, *JHEP* **08** (2019) 055, [[1807.09088](#)].
- [75] M. Abdughani, D. Wang, L. Wu, J. M. Yang and J. Zhao, *Probing the triple Higgs boson coupling with machine learning at the LHC*, *Phys. Rev. D* **104** (2021) 056003, [[2005.11086](#)].
- [76] M. Abdughani, K.-I. Hikasa, L. Wu, J. M. Yang and J. Zhao, *Testing electroweak SUSY for muon  $g - 2$  and dark matter at the LHC and beyond*, *JHEP* **11** (2019) 095, [[1909.07792](#)].
- [77] P. Athron, C. Balázs, D. H. J. Jacob, W. Kotlarski, D. Stöckinger and H. Stöckinger-Kim, *New physics explanations of  $a_\mu$  in light of the FNAL muon  $g-2$  measurement*, *JHEP* **09** (2021) 080, [[2104.03691](#)].
- [78] F. Wang, L. Wu, Y. Xiao, J. M. Yang and Y. Zhang, *GUT-scale constrained SUSY in light of new muon  $g-2$  measurement*, *Nucl. Phys. B* **970** (2021) 115486, [[2104.03262](#)].
- [79] M. Endo, K. Hamaguchi, S. Iwamoto and T. Kitahara, *Supersymmetric interpretation of the muon  $g - 2$  anomaly*, *JHEP* **07** (2021) 075, [[2104.03217](#)].
- [80] H. Baer, V. Barger, S. Salam, D. Sengupta and K. Sinha, *Status of weak scale supersymmetry after LHC Run 2 and ton-scale noble liquid WIMP searches*, *Eur. Phys. J. ST* **229** (2020) 3085–3141, [[2002.03013](#)].
- [81] F. Wang, W. Wang, J. M. Yang, Y. Zhang and B. Zhu, *Low energy supersymmetry confronted with current experiments: an overview*, [2201.00156](#).

- [82] J. Cao, C. Han, L. Wu, P. Wu and J. M. Yang, *A light SUSY dark matter after CDMS-II, LUX and LHC Higgs data*, *JHEP* **05** (2014) 056, [[1311.0678](#)].
- [83] J.-J. Cao, Z.-X. Heng, J. M. Yang, Y.-M. Zhang and J.-Y. Zhu, *A SM-like Higgs near 125 GeV in low energy SUSY: a comparative study for MSSM and NMSSM*, *JHEP* **03** (2012) 086, [[1202.5821](#)].
- [84] CMS collaboration, A. Tumasyan et al., *Search for higgsinos decaying to two Higgs bosons and missing transverse momentum in proton-proton collisions at  $\sqrt{s} = 13$  TeV*, [2201.04206](#).